STUDY OF NEUTRALIZATION-INDUCEDREINFORCING BAR CORROSION UNDER CYCLIC DRYING AND WETTING CONDITIONS

Lukuan QI Hiroshi SEKI Kotoyoshi TAKAGI

The performance of a reinforced concrete structure deteriorates gradually as corrosion of the reinforcing bars progresses. Understanding the rate at which reinforcing bars corrode is a prerequisite for calculating the performance of concrete structures. The main aim of this investigation is to study the corrosion rate of reinforcing bars using purpose-built models (a model for the control of corrosion by oxygen diffusion and one for control by specific resistance of the concrete). In order to obtain parameters to be used in the analysis of reinforcing bar corrosion, calculation models for water content and oxygen diffusion coefficient were formed using the distribution function of concrete pore size. In addition, accelerated corrosion experiments were performed on reinforcing bars embedded in neutralized concrete under cyclic drying and wetting conditions. The corroded mass of reinforcing bar embedded in neutralized concrete was quantitatively evaluated under cyclic drying and wetting conditions through using above-mentioned models and data function regressed from experiment. Comparing with experimental results, it is confirmed that these models for the corrosion of reinforcing bars are useful for the calculation of corroded mass.

Keywords: corrosion model, corrosion area, corroded mass, corrosion potential, specific resistance of concrete

Lukuan Qi graduated from Harbin University of Architecture and Engineering in 1985 and obtained a Dr. Eng. from Waseda University in 2001. His research interests relate to the durability of concrete and analytical approaches to RC structures.

Hiroshi SEKI is a Professor of Civil Engineering at Waseda University. He obtained a Dr. Eng. from the University of Tokyo in 1978. His research interests include the durability of concrete, the service life of RC members, and shear strength.

Kotoyoshi TAKAGI obtained a Master's Degree in Science and Technology from Waseda University in 1977 and is now General Manager of the Track and Structure Maintenance Section of the Facilities Department at East Japan Railway Company.

1. INTRODUCTION

Reinforced concrete structures are extremely durable and their service life is long enough that they are often regarded as permanent. However, cracking and flaking of cover concrete does occur, and this has become a problem for society. The main reason for these phenomena is corrosion of reinforcing bars embedded in the concrete. Expansive pressure resulting from such corrosion ultimately leads to cracking and flaking. After initial cracking, factors that cause corrosion easily penetrate the structure, and the reinforcing bar corrosion rate accelerates. This leads to loss of adhesion between the concrete and reinforcing bars, while the sectional area of the reinforcing bars is also reduced. Consequently, the functionality of the concrete structure deteriorates rapidly1).

In performing the durability design of reinforced concrete structures and carrying out their maintenance, the time-varying corrosion rate of the reinforcing bars must be fully understood if service life is to be accurately calculated. In general, reinforcing bars embedded in concrete corrode through salt damage and concrete neutralization, so the corrosion rate is related to the physical properties of the concrete. Concrete is a porous material, and its water content is closely related to natural environmental conditions. Moreover, the oxygen diffusion coefficient and specific resistance of the concrete directly affect the corrosion of reinforcing bars embedded in concrete, and these relate closely to the concrete's moisture state.

Typically, studies of reinforcing bar corrosion in concrete structures focus on corrosion properties and corrosion mass under constant environment conditions. In fact, however, concrete structures stand in a natural environment where changes in the physical properties of the concrete (water content, oxygen diffusion coefficient, specific resistance, etc.) and the state of reinforcing bar corrosion vary considerably with time.

The aim of this paper is to study the rate of reinforcing bar corrosion due to concrete neutralization. Models for the control of reinforcing bar corrosion by oxygen diffusion and specific resistance are constructed for a variable environment. So as to obtain parameters for use in analysis with the two models, the distribution function of concrete pore size is used and the calculation model of water content is formed. The change of water content in concrete inner is examined under cyclic drying and wetting conditions, and the calculation model of oxygen diffusion coefficient considered the change of water content is also assembled. Further, an accelerated corrosion experiment is carried out on reinforcing bars embedded in neutralized concrete under cyclic drying and wetting conditions. Changes in corrosion potential, corroded area of reinforcing bars, and corroded mass with the elapse of accelerated time are measured as part of the experiment. Change functions are calculated from the data obtained in the experiment. After obtaining these data and functions, an attempt is made to evaluate the corrosion mass of reinforcing bars embedded in neutralized concrete as well as the actual corrosion process under cyclic drying and wetting conditions.

2. CALCULATION MODELS FOR REINFORCING BAR CORROSION RATE

In the study, it is assumed that the environment varies from wetting conditions (high temperature and high humidity) to drying conditions (low temperature and low humidity), and these are adopted as the cyclic test conditions. Under wetting conditions, there is plenty of water in the concrete structure, and it is difficult for oxygen to diffuse from the concrete surface toward the core. This limits the amount of oxygen available for reinforcing bar corrosion, so the likelihood of oxygen diffusion being the controlling factor in reinforcing bar corrosion is higher. On the other hand, because the moisture content is low in the concrete core under drying conditions, the specific resistance of the concrete is higher and little corrosion current flows. As a result, the corrosion rate due to corrosion current is reduced, and the likelihood of specific resistance controlling corrosion becomes higher.

A study of specific resistance and oxygen diffusion during the corrosion of reinforcing bars embedded in mortar was performed by Saeki2). However, the evaluation of corrosion rate of reinforcing bars embedded in concrete is much more difficult in a general environment due to concrete neutralization. Based on the method described above, the corrosion rate of reinforcing bars embedded in concrete can be calculated using control models of oxygen diffusion and specific resistance.

(1) Model for oxygen diffusion control of corrosion

The model for oxygen diffusion control of reinforcing bar corrosion is described by Equation 2.13), 4). One of the problems with this equation is how to set the ratio of cathode to anode area.

In this study, the volume occupied by water and not occupied by water is assumed to be the anode and cathode, respectively, so the ratio of the two volumes is assumed to be the ratio of anode to cathode area. The water content and oxygen diffusion coefficient are calculated using the theoretical models of water content and oxygen diffusion coefficient described later in Section 3.

$$F_0 = \frac{k_{ri}^a}{k_{oi}^c}\cdot\frac{A_c}{A_a}\cdot\left[m\times S\times D\frac{dC(L,t)}{dL}\right] \qquad (2.1)$$

In which F_0 is the corrosion rate (g/cm^2·s), $k_{ri}{}^a$ and $k_{oi}{}^c$ are electrochemical equivalents, A_c is the cathode area, A_a is the anode area, m is oxygen solubility (cm^3/cm^3), S is water content (cm^3/cm^3), D is the oxygen diffusion coefficient (cm^2/s), and $C(L,t)$ is the oxygen concentration at the reinforcing bar position.

(2) Model for specific resistance control of corrosion

The upper surfaces of reinforcing bars embedded in neutralized concrete are assumed to form anode regions, while the lower surfaces form cathode regions. As shown in **Fig. 1**, it is assumed that corrosion current flows between the two regions and does not escape into the outer concrete, as demonstrated in past research[5), 6), 7)]. First, the potential distribution around a reinforcing bar is calculated using Equation 2.2, and then the current density at the interface between the corroded region and the non-corroded region is calculated. This current density is assumed to be the corrosion current density for specific resistance control.

$$\frac{\partial^2 P_v}{\partial x^2}+\frac{\partial^2 P_v}{\partial y^2}=0 \qquad (2.2)$$

$$F_{ri} = -\frac{P_{vi}}{\rho(S_r,T)} \qquad (2.3)$$

$$F_r = \sum_{1}^{n} F_{ri} \qquad (2.4)$$

In which F_r is corrosion current density (μA/cm), P_{vi} is potential at the interface (mV), P_v is the natural potential (mV), $\rho(S_r, T)$ is the specific resistance of the concrete (kΩ· cm), S_r is the relative water content (%), and T is temperature (°C).

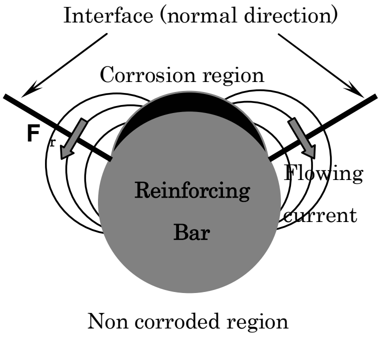

Fig.1 Specific resistance control model

The reinforcing bar corrosion rate can be calculated using these models. However, many parameters must be fixed for these analytical models. Calculations for water content and oxygen diffusion coefficient are described in the following Section 3, while natural potential, corrosion area, and specific resistance will be obtained from the experiments described in Section 4.

3. CALCULATION OF WATER CONTENT AND OXYGEN DIFFUSION COEFFICIENT

The water content of the core concrete changes under cyclic drying and wetting conditions, so the analytical parameters for reinforcing bar corrosion rate must also change. That is, the amount of oxygen and the specific resistance both vary. In this study, emphasis is placed on the concrete pore size distribution function in examining the changes in core concrete water content and the influence of oxygen diffusion and specific resistance.

(1) Calculation model for water content[8), 9), 10)]

a)Pore volume and distribution density function

Concrete pores occur in a wide range of diameters and forms in core concrete. In this study, only those pores that play an important role in moisture transport are considered. **Figure 2** shows the distribution function for pore capacity, which is expressed by Equations 3.1 and 3.2.

Pore volume function:

$$V_r = V_0\left[1-exp(-Br^C)\right] \qquad (3.1)$$

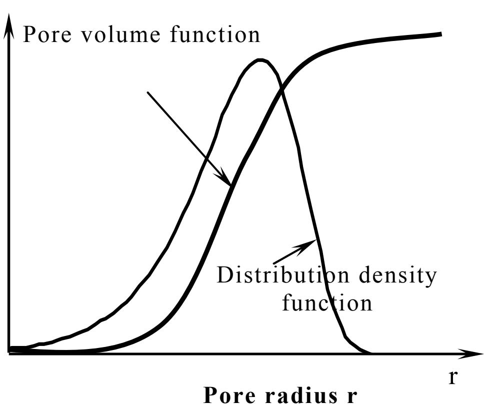

Fig.2 Definition of pore volume and distribution density function

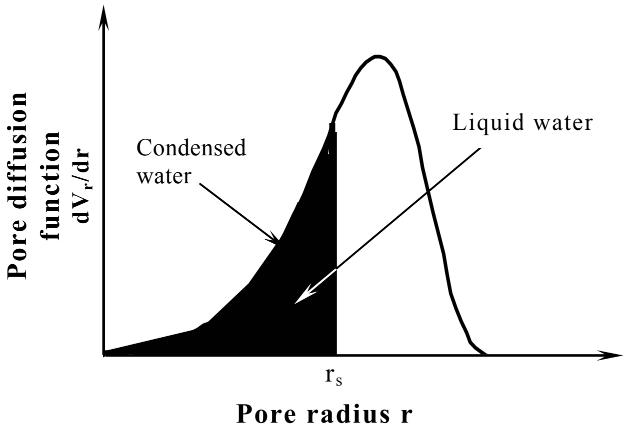

Fig.3 Moisture form in the pores

Density function of the pore volume distribution:

$$\frac{dV_r}{dr} = V_0 B C r^{C-1} \exp(-Br^C) \qquad (3.2)$$

In which V_r is the volume of pores of radius r (cm^3/cm^3), V_0 is the total pore volume (cm^3/cm^3), and B and C are parameters representing the function shape.

b) Equilibrium between water and vapor

As shown in **Fig. 3**, the pore structure is filled with an ideal gas mixture consisting of equilibrium levels of water and water vapor. The relationship between pore radius formed in gas-liquid interface and relative humidity is given by Kelvin's equation (Equation 3.3) because of the existence of vapor in the concrete.

$$\ln\frac{p_V}{p_{VO}} = -\frac{2\gamma_0 M}{RT\rho_w}\frac{1}{r_s} \qquad (3.3)$$

In which p_v is the partial pressure of vapor (Pa), p_{vo} is saturated aqueous vapor pressure (Pa), γ_0 is the surface tension of the liquid, M is the molecular weight of water (g/mol), R is the gas constant (J/mol·K), T is absolute temperature (K), and ρ_w is water density (g/cm^3).

c) Equation for water content

The maximum pore radius at which water exists in the liquid state can be calculated using Equation 3.3. It is assumed that if water fills pores up to radius r_s , the water content S of the concrete can be obtained from the following Equation 3.4.

$$S = \int_0^{r_s} dV_r = V_0\left[1 - \exp(-Br_s^C)\right] \qquad (3.4)$$

In which S is the water content (cm^3/cm^3) and r_s is the radius calculated from relative humidity.

(2) Calculation model for oxygen diffusion

It is assumed that concrete pores consist of cylinders of radius r. If the pressure is the same at both ends of the pore, gas movement consists of molecular diffusion, Knudson diffusion and surface movement[11), 12)]. Molecular diffusion and Knudson diffusion control the movement if the influence of surface movement is ignored.

When the ratio of radius r to mean free path λ of a gaseous molecule is greater than 10, the molecular diffusion coefficient D_n can be expressed by the following equation (Equation 3.5) if the mean molecular velocity equals c:

$$D_n = 1/3\bar{c}\lambda \qquad (3.5)$$

When the ratio of radius r to mean free path λ of the gaseous molecule is less than 0.1, molecular diffusion occurs, and the diffusion coefficient D_k is expressed by the following equation

(Equation 3.6):

$$D_k = 2/3\bar{c}r \qquad (3.6)$$

When the ratio of radius r to mean free path λ of the gaseous molecule is between 0.1 and 10, molecular diffusion and Knudson diffusion operate simultaneously. The diffusion coefficient D_m is then expressed by the following equation (Equation 3.7):

$$D_m = \frac{D_n}{(1+\lambda/2r)} \qquad (3.7)$$

As shown in **Fig. 4**, oxygen diffusion is mainly controlled by D_n when the pore radius is between 10λ and ∞, by D_m when the pore radius is from 0.1λ to 10λ, and by D_k from the oxygen molecular diameter d up to 0.1λ, respectively. Because gas transport theory is suitable for oxygen diffusion, the diffusion coefficient equations (Equations 3.5, 3.6, and 3.7) are suitable for use as a model for oxygen diffusion coefficient, and the oxygen diffusion coefficient D for concrete can be calculated using Equations 3.8, 3.9, and 3.10 by combining results for the different pore diameters present in the core concrete[13].

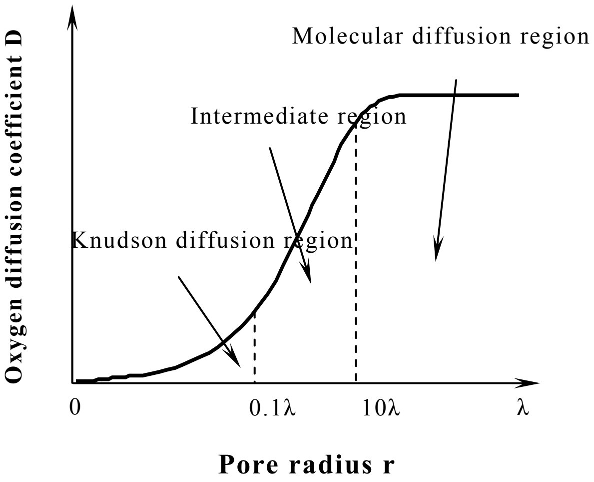

Fig.4 Definition of oxygen diffusion

$$D = \int_{r_s}^{0.1\lambda}\left(\frac{dV_k}{dr}\right)D_k dr + \int_{0.1\lambda}^{10\lambda}\left(\frac{dV_m}{dr}\right)D_m dr + \int_{10\lambda}^{\infty}\left(\frac{dV_n}{dr}\right)D_n dr \qquad \text{for } d \le r_s \le 0.1\lambda \qquad (3.8)$$

$$D = \int_{r_s}^{10\lambda}\left(\frac{dV_m}{dr}\right)D_m dr + \int_{10\lambda}^{\infty}\left(\frac{dV_n}{dr}\right)D_n dr \qquad \text{for } 0.1\lambda \le r_s \le 10\lambda \qquad (3.9)$$

$$D = \int_{r_s}^{\infty}\left(\frac{dV_n}{dr}\right)D_n dr \qquad \text{for } r_s \ge 10\lambda \qquad (3.10)$$

In which D is the oxygen diffusion coefficient (cm^2/s), $D_{k,m,n}$ is the diffusion coefficient for each range (cm^2/s), and dV_k/dr, dV_m/dr, and dV_n/dr are the distribution densities of pores in each range (cm^3/cm^3.cm).

Besides, the mean molecular velocity c and mean free path λ are expressed by Equations 3.11 and 3.12.

$$\bar{c} = \sqrt{\frac{8RT}{\pi M}} \qquad (3.11)$$

$$\lambda = \frac{RT}{N\pi d^2 P} \qquad (3.12)$$

In which M is the molecular weight of water (g/mol), R is the gas constant (J/mol·K), P is gas pressure (Pa), N is a coefficient, T is absolute temperature (K), and d is the diameter of an oxygen molecular (cm).

Changes in water content and oxygen diffusion coefficient in the core concrete with the elapse of time can be calculated using the models described in this section. The corrosion rate of reinforcing bars can then be calculated using models of reinforcing bar corrosion taking account of variations in these parameters as obtained from Section 2.

4. REINFORCING BAR CORROSION EXPERIMENT

In order to obtain the parameters to be used in the calculation models for reinforcing bar corrosion rate, an accelerated experiment is performed to determine the corrosion of reinforcing bars embedded in neutralized concrete. That is, an effort is made to understand the corrosion characteristics of reinforcing bars embedded in concrete under cyclic drying and wetting conditions once neutralization has taken place. To this end, the reinforcing bar natural potential, corrosion area, corroded mass, and changes in specific resistance are measured as time elapses, and the relationship between these measurements and accelerated time is studied.

(1) OUTLINE OF EXPERIMENT

a) Outline of experimental specimens

Table 1 gives details of the materials employed and **Table 2** shows the mix proportions used for the experimental specimens. Specimens for reinforcing bar corrosion and specimens for specific resistance were manufactured as shown in **Figs. 5** and **6**. Reinforcing bars were soaked in 10% citric acid ammonium solution to remove the oxide film prior to specimen manufacture, then placed in a 70 x 70 x 200 mm mold ready for concrete placement. Concrete casting was from bottom to top as shown in the figures. Specimens were demolded at the first day and were then cured in water until the age of seven days. Afterwards, they were placed in an indoor environment at a temperature of 20°C and a relative humidity of 60%, with all surfaces except the accelerated neutralization surface covered with epoxy resin to prevent the ingress of components from the environment. The reinforcing bars were 200 mm in length and the cover was 15 mm.

In order to measure electrical resistance and concrete water content, two kinds of specimen were made. The electrode area was 40 x 40 mm and electrode spacing was 30 mm.

Table 1 Material properties

Cement	Ordinal portland cement
Fine aggregate	River sand (Density2.58g/cm^3, Fineness Modules 3.16)
Coarse aggregate	Crushed stone (Density 2.63g/cm^3, Fineness Modules 6.52) Maximum size 10mm
Admixture	AE water reducing agent
Reinforcing	SR45 ϕ9mm

Table 2 Mix proportioning

Slump (cm)	Air content (%)	W/C (%)	Quantity of material per unit volume of concrete (kg/m^3)				AE water reducing agent (ml)
			Cement	Water	Fine aggregate	Coarse aggregate	
8±0.5	8±0.5	70	260	182	926	785	662

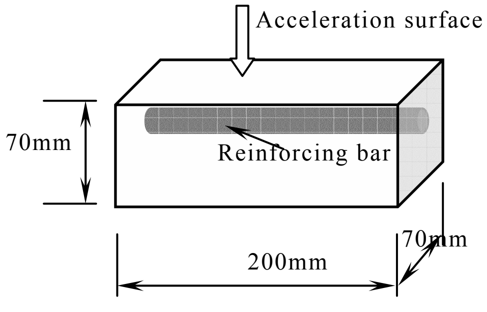

Fig.5 Size of specimen for reinforcing bar corrosion

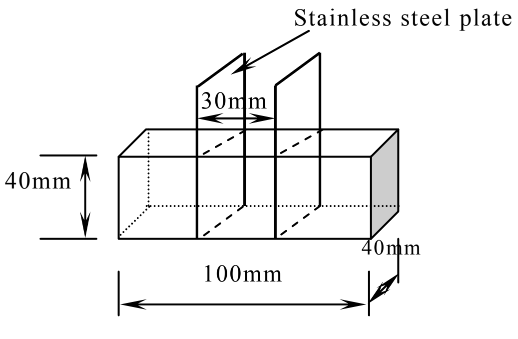

Fig.6 Size of specimen for specific resistance

b) Accelerated neutralization and corrosion conditions

Each experimental specimen was moved into the accelerated neutralization test equipment at the age of 14 days. Accelerating conditions were a temperature of 40°C, a relative humidity of 50%, and a CO_2 concentration of 10%. Concrete specimens identical to the corrosion specimens containing reinforcing bars were cut open with a diamond cutter to measure neutralization depth using 10% solution of phenolphthalein in alcohol as neutralization progressed. When the neutralization depth reached 15 mm (age of 29 days), 19 mm (age of 35 days), and 23 mm (age of 43 days), respectively, reinforcing bar corrosion specimens were removed from the accelerated test neutralization equipment and placed in the accelerated corrosion test equipment. Neutralization depths of 15, 19, and 23 mm meant that neutralization had reached the upper surface, center, and lower surface of the reinforcing bars, respectively. Cyclic drying and wetting was carried out in the accelerated corrosion test. The cycle consisted of one week of high temperature and high humidity, then one week of low temperature and low humidity, continuing for a period of 20 weeks.

c) Measurement method

The natural potential of specimens undergoing the accelerated corrosion test was measured at 0, 2, 4, 6, 7, 12, 16, and 20 weeks. Each specimen was soaked in water for 24 hours before potential measurement, then a wet sponge was placed on the measurement surface and the natural potential was measured. The reference electrode was a saturated calomel electrode (SCE).

Three specimens were fractured at each accelerating week, and the reinforcing bar removed after measurement of the natural potential at the 4, 8, 12, and 20 week points. The corrosion area and loss were then measured. The area of corrosion was rapped with cellophane and was sketched with magic pen. Afterward, the corrosion area was calculated using a dot counting program. This yielded the ratio of corroded area of the reinforcing bar. Moreover, the corroded mass was calculated using Equation 4.1 after removing the rust with 10% ammonium hydrogen citrate solution. In order to remove the influence of the passive film in the non-corroded region, the weight loss of a non-corroded reinforcing bar was measured and the result was used for correction.

$$\Delta W = \left(W_0 - W\right) - W_p \times \frac{100 - A}{100} \qquad (4.1)$$

In which Δw is corroded weight (mg), w_0 is the reinforcing bar weight before casting (mg), W is the reinforcing bar weight after removing the rust (mg), W_p is the weight loss in a non-corroded region (mg), and A is the ratio of corroded area (%).

The specific resistance was measured using a specimen of the same age produced specially for specific resistance measurements. Specific resistance can be calculated using Equation 4.2, and the relative water content is obtained from Equation 4.3. The method of measurement was to take the specimen weight at a particular age, obtain the saturated weight after soaking in water for three days, and then obtain the dry weight after drying (at a temperature of 105°C) for three days.

$$\rho = \frac{Z \times A_s}{h} \qquad (4.2)$$

$$S_r = \frac{m_t - m_d}{m_s - m_d} \times 100\% \qquad (4.3)$$

In which ρ is the specific resistance of the concrete (Ω·cm), S_r is the relative water content (%), Z is the real number component of impedance at a frequency of 1 kHz (Ω), A_s is the area of the stainless steel plates embedded in the concrete (cm^2), h is spacing between the two stainless steel plates (cm), m_c is the test weight (mg), m_s is the saturated weight (mg), and m_d is the dry weight (mg).

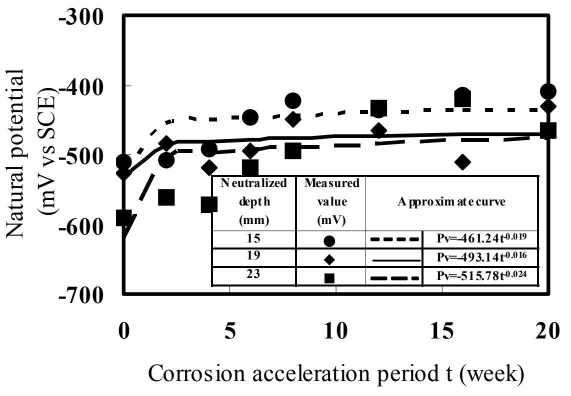

Fig.7 Change in natural potential

(2) Experimental results

a) Progression of reinforcing bar corrosion

Figure 7 shows changes in the natural potential of reinforcing bars embedded in neutralized concrete with the elapse of time. The natural potential is less noble as a consequence of concrete neutralization, and has nothing to do with variations in carbonation depth. It tends to become slightly noble as accelerated time passes, and after an accelerated period of 8 weeks the change becomes less rapid. These results agree in general with the results reported by Saeki(2). The change in natural potential with the elapse of accelerated time can be expressed by Equation 4.4.

$$P_v = P_{vo} t^{-\alpha} \qquad (4.4)$$

In which P_v is natural potential at accelerated time t, P_{vo} is natural potential before accelerated corrosion (mV), α is a coefficient, and t is accelerated time period (weeks).

The regression parameters of natural potential for different neutralization depths are shown in **Fig. 7**. Natural potential differs depending neutralization depth at the beginning stage of the experiment.Although the variance of coefficient α is not large regarding neutralization depth, it is admitted in this experiment that the neutralization depth influences natural potential of reinforcing bar corrosion. The natural potential of reinforcing bars embedded in non-neutralized concrete was measured using other specimens at the same time, and was found to be approximately -154 mV (denotated as to SCE).

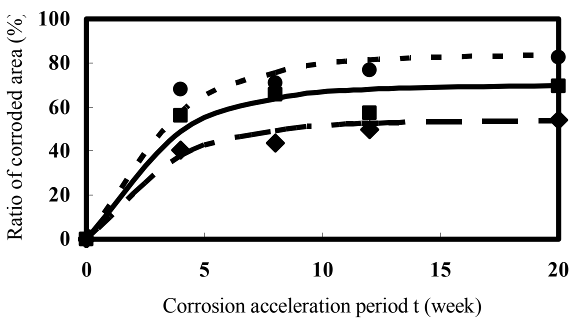

Fig.8 Change in ratio of corroded area

Figure 8 shows changes in the corroded area ratio of a reinforcing bar. Greater change is seen in the first four weeks of accelerated time for various neutralization depths, while after four weeks the change become sluggish. The corroded area is 50% for a neutralization depth of 15 mm, 70% for 19 mm, and 80% for 23 mm after 20 weeks of accelerated time. The change in corroded area ratio with time is described by Equation 4.5, described in **Fig. 8**.

$$A = A_0 (1 - 10^{\beta \times t}) \qquad (4.5)$$

In which A is the ratio of corroded area at accelerated time t (%),

Notarization depth 15mm (◆)

$$A = 54.2 \times (1 - 10^{-0.131t})$$

Notarization depth 19mm (■)

$$A = 71.1 \times (1 - 10^{-0.127t})$$

Notarization depth 23mm (●)

$$A = 84.01 \times (1 - 10^{-0.125t})$$

A_0 is the ratio of corroded area at an accelerated time of 20 weeks (%), β is a coefficient, and t is accelerated time period (week).

The state of reinforcing bar corrosion after an accelerated time period of 20 weeks is shown in **Fig. 9**. Variations in corrosion state in the axial direction are small, and the damage is not pit corrosion. A cross-sectional view of the corrosion state is also shown in **Fig. 9**. Corrosion is particularly evident on the upper and lower surfaces of the reinforcing bar. This confirms

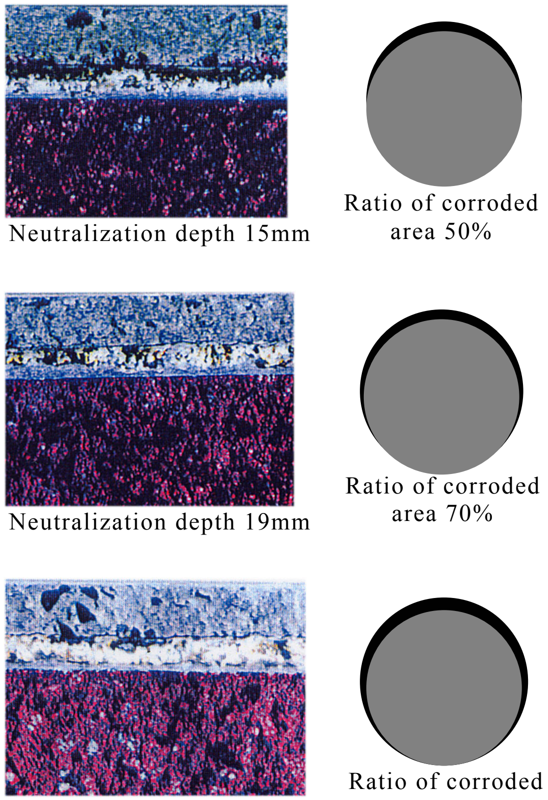

Neutralization depth 15mm

Ratio of corroded area 50%

Neutralization depth 19mm

Ratio of corroded area 70%

Neutralization depth 23mm

Ratio of corroded area 80%

(a) Measured

(b) Sectional corrosion

Fig.9 Corroded state of reinforcing bars (20 weeks)

that neutralization depth has a great influence on the ratio of reinforcing bar corrosion. That is, neutralization depth influences the initial natural potential of a reinforcing bar and also its corroded area.

(b) Changes in specific resistance of concrete

The relationship between specific resistance and relative water content is shown in **Fig. 10**. Specific resistance can thus be expressed in terms of relative water content, as given by Equation 4.6. The values of ρ_s and coefficient γ in this equation are described in **Fig. 10**.

$$\rho_s = \rho_0 S_r^{-\gamma} \qquad (4.6)$$

In which ρ_s is specific resistance (kΩ•cm), ρ_0 is a coefficient (kΩ•cm), S_r is relative water content (%), and γ is a coefficient.

Specific resistance is influenced by the pore structure, mortar content, and temperature as well as the relative water content mentioned above. However, since the mix was constant in this experiment, only the influence of temperature needs to be considered. A temperature correction for specific resistance was performed with reference to another study$^{14)}$, as expressed by Equation 4.7.

$$\rho_T = 2.5 \times 10^{-0.02T} \qquad (4.7)$$

In which ρ_T is the temperature correction coefficient based on resistance at 20˚C and T is temperature (˚C).

The final expression for specific resistance is then given by Equation 4.8.

$$\rho(S_r, T) = \rho_S \rho_T \qquad (4.8)$$

In which $\rho(S_r,T)$ is the specific resistance of the concrete at relative water content S_r and temperature T.

5. CALCULATION OF REINFORCING CORROSION PROCESS

In this section, analytical parameters are selected using the models of concrete water content and oxygen diffusion coefficient described in Section 3, as well as the experimental results relating to reinforcing bar corrosion described in Section 4. Then the calculation models (for oxygen diffusion control and specific resistance control) of reinforcing bar corrosion described in Section 2 are used to analyze the corrosion process of reinforcing bars embedded in neutralized concrete.

(1) Analytical conditions

The finite element method is used to calculate the corrosion rate of reinforcing bars. The analytical results are compared with the results of the accelerated experiment.

In the model for oxygen diffusion control of corrosion, the analytical mesh is quadrilateral throughout, and the ingress of water vapor and oxygen is limited to the uncoated surface; ingress from coated surfaces is assumed to be zero.

In the model for specific resistance control of corrosion, the regression equation (Equation 4.4) for natural potential change with time, as described in Section 2, is assumed to give the potential change in the corrosion region. In

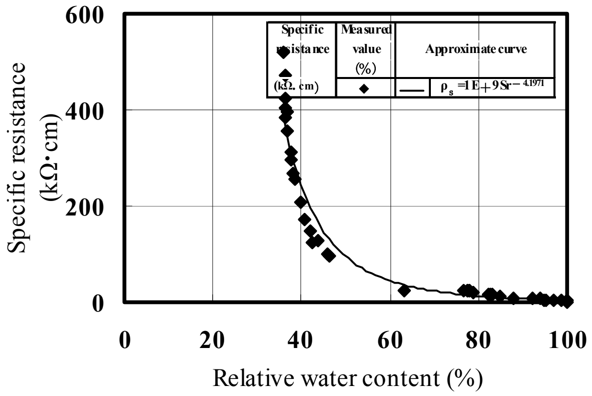

Fig.10 Relationship between relative water content and specific resistance

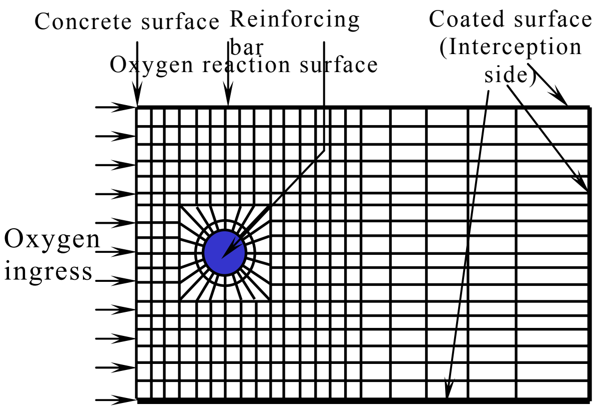

Fig.11 Finite element division used for analysis

other words, the measured natural potential is taken to be the potential of the corroded region (upper surface of reinforcing bar), while the natural potential of a reinforcing bar embedded in non-neutralized concrete measured using an independent specimen is taken as the natural potential of the un-corroded region (bottom surface of reinforcing bar). The analytical mesh is similar to that shown in **Fig. 11**. It is quadrilateral throughout and the maximum mesh size is 0.5 mm. The parameters of the pore distribution function described in Equation 3.1 are used for analysis, while the diffusion coefficient describing water vapor movement is taken from a past study[7)]. **Table 3** shows these parameters. The diffusion coefficient for water vapor is assumed to be constant throughout the process of reinforcing bar corrosion under cyclic drying and wetting.

Table 3 Parameters used for analysis

V_0(cm^3/cm^3)	0.172
B	22400
C	0.5
Solubility of oxygen (cm^3/cm^3)	0.034(15°C)
	0.023(40°C)
Steam diffusion coefficient(cm^2/s)	2.627($\times 10^{-5}$)

(2) Comparison of analysis and experiment

The calculation procedure for corrosion rate and corrosion mass is described in **Fig. 12**. Analytical results for water content and oxygen diffusion coefficient are shown in **Table 4** for cyclic drying and wetting conditions. This table confirms that the water content of the core concrete reaches a maximum under high temperature and high humidity conditions and a minimum under low temperature and low humidity conditions. On the other hand, the law governing oxygen diffusion coefficient is the opposite. The change in corroded mass with elapse of accelerated time is shown in **Figs. 13** and **14** for a neutralization depth of 23 mm. **Figure 13** includes the analytical result based on the model for oxygen diffusion control of corrosion, while **Fig.14** includes the analytical result based on the specific resistance control model. The results indicate a monotonic rise, and in this sense they are similar to the experiment results from **Fig. 13**. However, the analytical values greatly exceed the experimental values. This means that the possibility of oxygen diffusion alone controlling corroded mass is very low for the accelerated period analyzed. The corroded mass follows the same general trend as the experimental values in **Fig. 14**, and the analysis yields higher values. The discrepancy increases with the elapse of accelerated time. In the accelerated experiment described in Section 2, the cyclic period of high temperature and high humidity (temperature of 40˚C; humidity of 95%) is one week, and this is followed by one week of low temperature and low humidity. As a result, the likelihood of reinforcing bar corrosion being controlled alternately by oxygen diffusion and specific resistance is high.

Figure 15 shows the analytical results obtained by using the model for oxygen diffusion control and the model for specific resistance control. The corroded weight as calculated by the model for oxygen diffusion control is smaller than that using the model for specific resistance control during the one-week periods of high temperature and high humidity. On the other hand, the opposite is true in the low temperature and low humidity cycle. Because there is a plentiful supply of moisture in the core concrete under high temperature and high humidity conditions, it is difficult for oxygen to enter the core concrete, and demand oxygen for corrosion reaction is smaller. As a consequence, reinforcing bar corrosion is controlled by oxygen diffusion due to the limited supply oxgen. On the other hand, the moisture supply is limited under conditions of low temperature and low humidity, so the specific resistance is higher. As a result, the flow of corrosion current is very restricted, and reinforcing bar corrosion is controlled by specific resistance. Summarizing these results, it is presumed that oxygen diffusion controls corrosion under conditions of high temperature and high humidity, while specific resistance is the controlling factor under low temperature and low humidity conditions. These results are in agreement with past studies[2), 15)].

As above discussed, the analytical value has to be controlled either oxygen diffusion or specific resistance. Fig.15 indicated the corrosion weight of reinforcing bars based on both oxygen diffusion model and specific resistance model. If is clear from Fig.15 that corrosion weight for

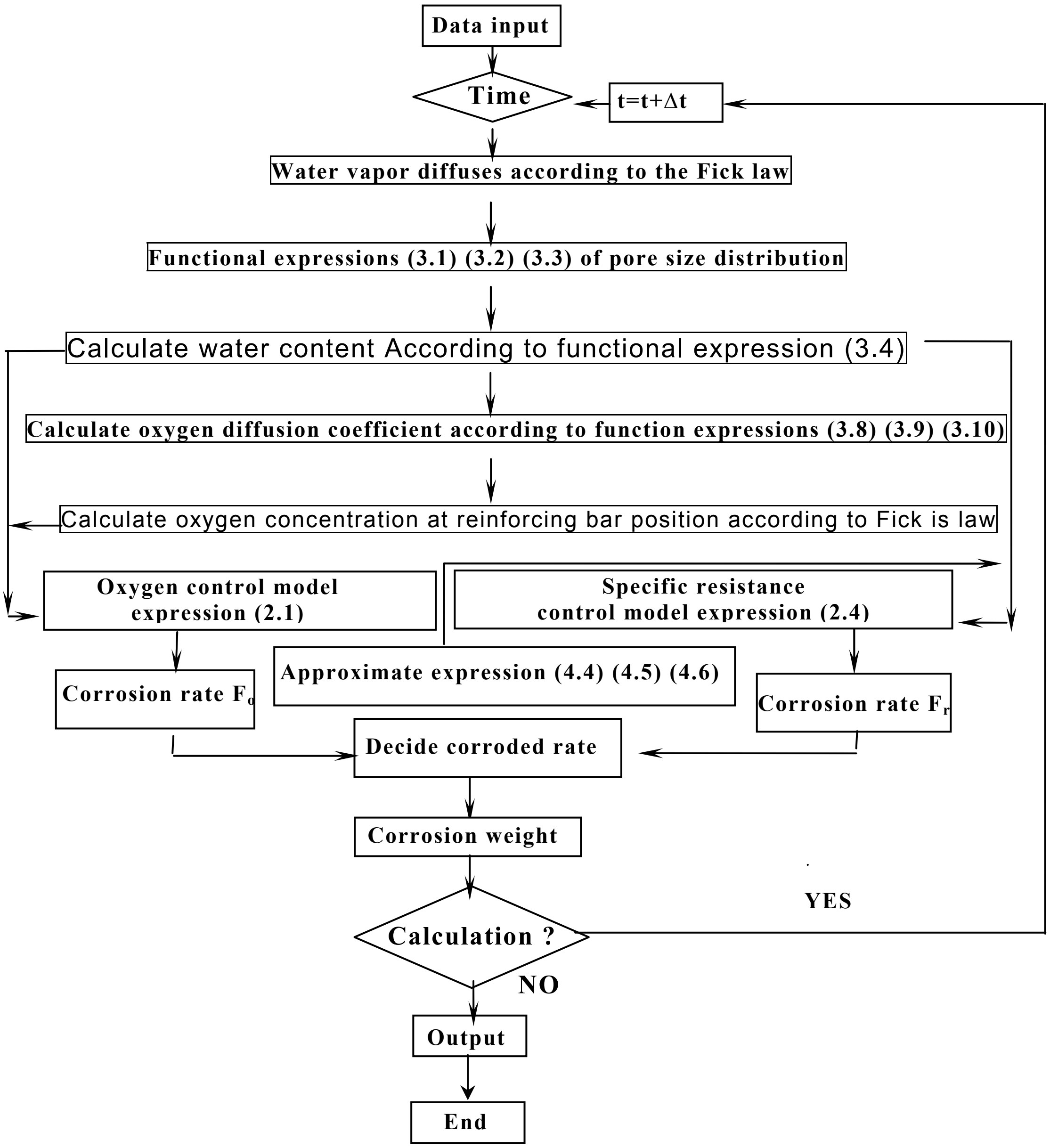

Fig.12 Calculation produce for corroded weight of reinforcing bar

Table 4 Calculation results

Calculation condition	Water content (cm^3/cm^3)	Oxygen diffusion coefficient (cm^2/s)
High temperature and high humidity	0.162 (Maximum)	5.70×10^{-4} (Minimum)
Low temperature and low humidity	0.095 (minimum)	1.33×10^{-3} (maximum)

corrosion weight calculated from the model for oxygen diffusion control is assumed to be the actual corrosion mass under accelerated conditions of high temperature and high humidity. Similarly, the corroded mass calculated from the model for specific resistance control is assumed to be the actual corroded mass under accelerated conditions of low temperature and low humidity. The relationship between corroded mass and accelerated corrosion time can be obtained by adding the corroded mass during each cycle of the above accelerated conditions.
The analytical and experimental values for corroded mass of reinforcing bars are shown in **Figs.**

16, 17, and **18** for specimens with neutralization depths of 15, 19, and 23 mm, respectively. The corroded mass increases almost linearly in the case of the analytical results, reflecting the experiment results obtained by Saeki and Morinaga[2),16)]. This confirms that the analytical method described for reinforcing bar corrosion in neutralized concrete is basically reasonable. However, although the analytical results reflect the overall change trends in **Figs. 17** and **18**, there is some discrepancy with the experimental results. The main reason for this is that in constructing the model or specific resistance control, the influence of reinforcing bar polarization resistance was not considered, and the flow of current in the rust layer was not taken into account.

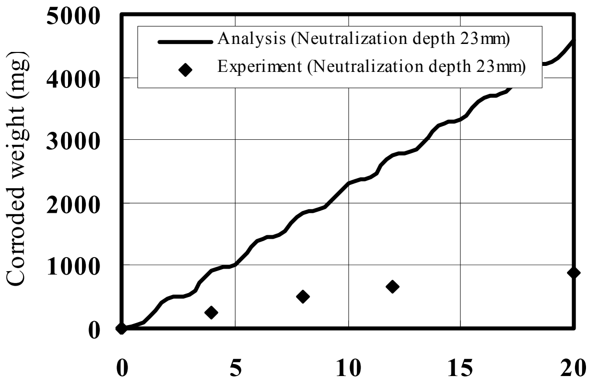

Fig.13 Relationship between accelerated period and corroded weight (Oxygen control model)

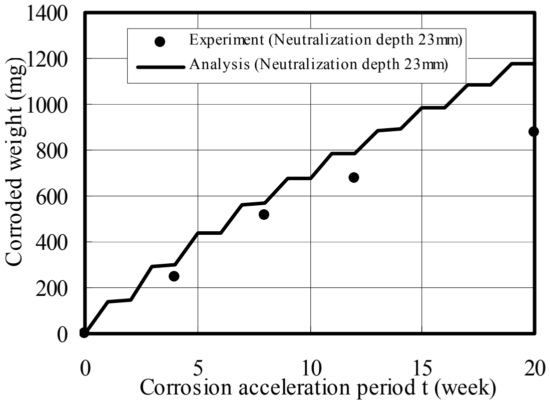

Fig.14 Relationship between accelerated period and corroded weight (Specific resistance control model)

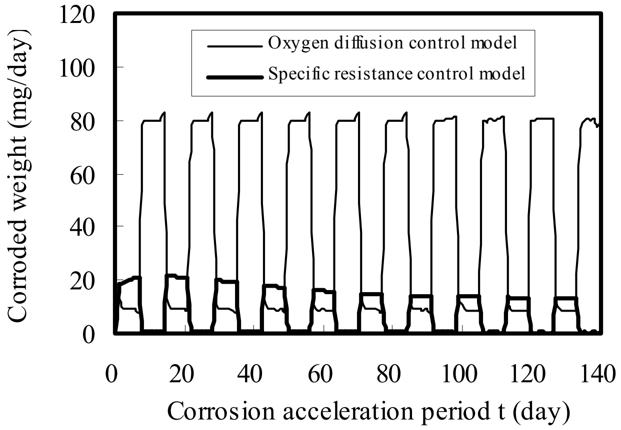

Fig.15 Comparison of corroded weight

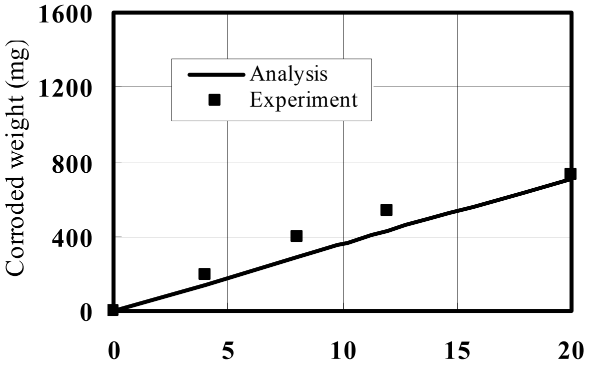

Fig.16 Change in corroded weight (Neutralization depth 15mm)

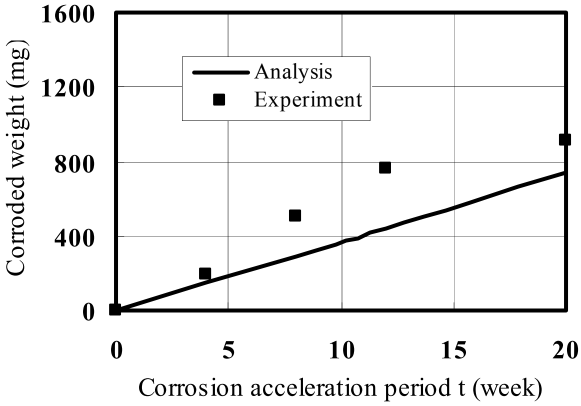

Fig.17 Change in corroded weight (Neutralization depth 19mm)

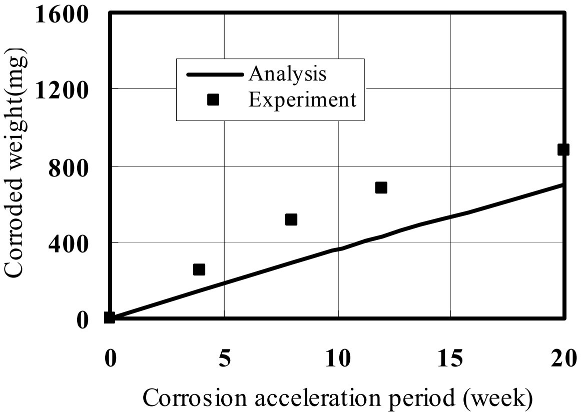

Fig.18 Change in corroded weight (Neutralization depth 23mm)

6. CONCLUSIONS

The aim of this research was to clarify the corrosion characteristics of reinforcing bars embedded in neutralized concrete under alternate drying and wetting conditions. A calculation model for the corrosion rate of reinforcing bars was constructed on the basis of a proposed method. The respective volumes occupied by water and not occupied by water in the core concrete are treated as the anode and cathode in the model for oxygen diffusion control of corrosion, so the ratio of the two volumes is assumed to be the area ratio of anode to cathode. The current density at the interface between corroded and non-corroded regions is obtained, and this current density is taken as the corrosion current in the model for specific resistance control of corrosion. In order to obtain suitable parameters for use in the corrosion model, calculation models for water content and oxygen diffusion coefficient were constructed, and also concrete specimens were manufactured with embedded reinforcing bars for use in an accelerated experiment to measure reinforcing bar corrosion in neutralized concrete specimens. Finally, finite element analysis was carried out using the models. The following conclusions can be drawn from the results:

(1) The natural potential of a reinforcing bar varies with neutralization depth. The natural potential becomes more negative as neutralization progresses.

(2) The ratio of corroded area of a reinforcing bar varies with neutralization depth. The corroded area increases as neutralization progresses.

(3) Pinhole corrosion resulting from neutralization was not evident on reinforcing bars. Rather, the surface of reinforcing bars was evenly corroded.

(4) The analytical results using the models for oxygen diffusion control and concrete specific resistance control confirm that corrosion is controlled by oxygen diffusion under conditions of high temperature and high humidity, while it is controlled by specific resistance of the concrete at low temperature and low humidity.

(5) The corroded mass of a reinforcing bar can be calculated by selecting calculation values based on the more suitable of the two corrosion models, depending on the natural potential, the corrosion area ratio, and specific resistance, and using the calculation models for water content and oxygen diffusion coefficient. This makes it possible to calculate the corrosion rate of reinforcing bars in neutralized concrete under cyclic drying and wetting conditions.

The analysis of reinforcing bar corrosion was carried out using equations regressed from experimental data. In order to obtain a universal method of calculating parameters for use in the corrosion model, it will be necessary to accumulate data from existing concrete structures as well as from further experiments.

Acknowledgement

The authors gratefully acknowledge the valuable contribution made to this study by Mr. K. Ishizawa and Mr. L. Iwata, and they also thank the members of the corrosion and corrosion prevention subcommittee of the concrete committee for their kind and valuable advice.

References

1)Sub-committee on Corrosion and Corrosion-Protection: Resent State and Future Tendency on Corrosion Protection and Repair, Concrete Committee of Japan Society of Civil Engineers, 1997
2)Tatuhiko Saeki, Nobuaki Daisoku, and Sigeyosi Nagataki: Quantitative Estimation of steel corrosion in mortar due to carbonation, Proceedings of the Japan Society of Civil Engineers No.532/ V-30 pp.55-66 1996
3)Hiroshi Seki and Hideo Yamamoto: Analytical Approach to Corrosion Rate of Bars Embedded in Reinforced Concrete, Proceedings of the Japan Concrete Institute, Vol.9, No.1, pp.381-386, 1987
4)Report of Research Committee: Research on Complex Theme of Structure and Durability of Reinforced Concrete Members, Japan Concrete Institute, 1998
5)Rie Oyama, Tetuzi Yazima, Takehito Uomoto, and Tomio Hoshino: Prediction of Steel Corrosion Portion and Area Natural Potential Measurement, Proceedings of the Japan Society of Civil Engineers No.550 /V-34 pp.13-21 1996
6)Masahiko Otomaru and Masayasu Otu: Evaluation of Bar Corrosion Based on Method of Natural Electric Potential by way of Three-dimensional BEM Analysis, Proceedings of the Japan Concrete Institute, Vol.2, No.1, pp.539-544, 1990
7)Masayasu Otu and Hironori Yamamura: Evaluation of Bar Corrosion Based on Method of Natural Electric Potential by way of CSM Analysis, Proceedings of the Japan Concrete Institute, Vol.3, No.1, pp.527-532, 1991
8)Takumi Simomura and Kazumasa Ozawa: Analysis of Water Movement in Concrete Based on Capillary Structure Model, Proceedings of the Japan Concrete Institute Vol.4 No.1 pp.631-636, 1992
9)Takumi Simomura and Kouichi: Drying Shrinkage Aging Model of Concrete Based on Micromechanisms in Concrete, Proceedings of the Japan Society of Civil Engineers No.520/ V-28 pp.35-45, 1995
10) Tetuya Isida, Rajesh P.Chaube ,Toshiharu Kishi, and Kouichi Maekawa: Modeling of Pore Water Content in Concrete Under Generic Drying-Wetting Conditions, Proceedings of the Japan Society of Civil Engineers No.564/ V-35 pp.199-209 1997
11) Yves F.Houst: Influence of Porosity and Water Content on the Diffusivity of CO_2 and O_2 through Hydrated Cement Paste, Cement and Concrete Research, Vol.24, No.6, pp.1165-1176, 1994
12) Kazusuke kobayashi and Keizou Syutou: Properties of Oxygen Diffusion Through Cementitious Materials, Concrete Technology, Vo.24, No.12, pp.91-106, 1986
13) Sudjono A .S and Hiroshi Seki: Properties of Gas Diffusion Through Concrete, Transactions of Conference on Cement and Concrete, V25, pp.83-88, 1998
14) Hironobu Ono, Sakithi Oogisi, and Ken Bun: Influence of Testing Conditions and Applied Stress on Electrical Resistance of Concrete, Proceedings of the Japan Concrete Institute, Vol.3, No.1, pp.411-446, 1991
15) Michio Oozumi and Takehito Uomoto: Prediction Method for Corrosion Rate of Reinforcing Bar in Concrete Based on Oxygen Diffusion Theory, Proceedings of the Japan Society of Civil Engineers, No.648/V-47, pp.1-8, 2000
16) Sigeru Morinaga: Estimation of Service Life of Reinforced Concrete Building Based on Corrosion Rate of Bars, Research Report of Shimizu Corporation, No.23, 1986